Journal of the Mechanical Behavior of Biomedical Materials 173 (2026) 107221

Contents lists available at ScienceDirect

Journal of the Mechanical Behavior of Biomedical Materials

journal homepage: www.elsevier.com/locate/jmbbm

Increasing the fatigue strength of laser-powder bed fusion manufactured Ti6Al4V hip stems by means of appropriate post-treatments

Stefan Schroeder [a,*,1], Jens Gibmeier [b,1], Phuong Thao Mai [b], Maximilian C.M. Fischer [c], Moritz M. Innmann [a], Tobias Renkawitz [a], J. Philippe Kretzer [a]

[a] Research Center of Biomechanics and Implant Technology, Department of Orthopaedics, Heidelberg University Hospital, Schlierbacher Landstraße 200A, 69118, Heidelberg, Germany
[b] Institute for Applied Materials, Karlsruhe Institute of Technology, 76131, Karlsruhe, Germany
[c] AQ Solutions GmbH, An der Hasenkaule 10, 50354, Hürth, Germany

ARTICLE INFO

Keywords:
Polishing
Shot peening
Residual stress
Additive manufacturing
Orthopedic implants

ABSTRACT

Due to the lower fatigue resistance of LPBF manufactured Ti6Al4V alloy compared to wrought material, hip stems are still manufactured conventionally, despite the advantages of patient-specific joint replacements. Therefore, the aim of the study was the investigation of appropriate post-treatments to increase the fatigue resistance of LPBF manufactured Ti6Al4V alloy using a four-point bending setup and a Locati-test. The results showed that only a combination of a hot isostatic pressing process and a sufficient surface treatment can lead to similar fatigue results as wrought material. Thereby, machining, deep rolling and shot peening turned out to be suitable surface treatments. For complex geometries like hip stems, shot peening is the most sufficient surface treatment. A combined surface treatment of shot peening and polishing led to similar fatigue results as the shot peening process alone. It can be followed that a combination of shot peening with a previous hot isostatic pressing process leads to satisfying fatigue results comparable to the wrought material and can be applied on complex geometries like hip stems. In addition, shoulder and neck area of a hip stem can be polished after the HIP process and the shot peening procedure without any reduction in fatigue strength.

1. Introduction

The laser-powder bed fusion (LPBF) additive manufacturing (AM) technology is already an inherent part of orthopedic interventions worldwide (Lal and Patralekh, 2018). Especially the possibility to customize 3D-manufactured implants is a main advantage of AM in orthopedics (Wixted et al., 2021). Well-established examples of 3D-manufactured implants with good mid-term results are spinal cages, acetabular cups, and pelvic implants to replace bony defects (Chen et al., 2020; Dall'Ava et al., 2019; Jin et al., 2021; von Hertzberg-Boelch et al., 2021). The titanium alloy Ti6Al4V is the material of choice for bony contact, due to its excellent biocompatibility, corrosion resistance and elasticity, which is closer to the elasticity of cortical bone than alternative biocompatible metallic materials with sufficient mechanical strength (Chen and Thouas, 2015). The possibility of manufacturing complex geometries and porous structures from Ti6Al4V powder were key advantages to process cement free implants, showing a strong osseointegration (Dall'Ava et al., 2021; Ren et al., 2021). Similar to the conventional i.e. subtractive manufacturing processes like machining processes, the manufacturing of Ti6Al4V by LPBF showed a good biocompatibility in in vivo and in vitro tests (Wang et al., 2016). In addition, the elasticity modulus can be adjusted to the bone by manufacturing implants with a specific porosity to reduce stress shielding processes (Chen et al., 2017). The main disadvantage of LPBF-processed Ti6Al4V implants however, is the reduced fatigue resistance compared to conventional shaping and subtractive manufacturing processes, such as forging, casting, or machining (Strantza et al., 2016). Different factors can be mentioned, which lead to

* Corresponding author. Research Center of Biomechanics and Implant Technology, Department of Orthopaedics, Heidelberg University Hospital, Germany, Schlierbacher Landstraße 200a, 69118, Heidelberg, Germany.
E-mail addresses: Stefan.Schroeder@med.uni-heidelberg.de (S. Schroeder), Jens.Gibmeier@kit.edu (J. Gibmeier), Phuong.Mai@kit.edu (P.T. Mai), Maximilian.Fischer@aq-solutions.de (M.C.M. Fischer), Moritz.Innmann@med.uni-heidelberg.de (M.M. Innmann), Tobias.Renkawitz@med.uni-heidelberg.de (T. Renkawitz), Philippe.Kretzer@med.uni-heidelberg.de (J.P. Kretzer).
[1] the authors Stefan Schroeder and Jens Gibmeier contributed equally to this work.

https://doi.org/10.1016/j.jmbbm.2025.107221
Received 11 September 2024; Received in revised form 19 September 2025; Accepted 30 September 2025
Available online 6 October 2025

a reduction of the fatigue resistance of AM processed Ti6Al4V specimens. First, the pronounced surface roughness, which is beneficial for the osseointegration, may be a predetermined breaking point, from which a crack could arise due to the notch effect. Secondly, the AM process leads to a specific porosity in the material, which depends on the LPBF process parameters and the sample dimensions (du Plessis, 2019; Zhao et al., 2016). A study by Leuders et al. showed, that the pores in AM processed specimens are a key factor of a reduced fatigue behavior (Leuders et al., 2013). Thirdly, comparing the microstructure of LPBF processed Ti6Al4V and conventionally manufactured Ti6Al4V samples differences can be found. According to Kasperovich and Hausmann, the microstructure of the wrought material is a α-globular phase in an $\alpha + \beta$ matrix, whereby the LPBF printing process leads to an acicular martensitic phase, which is hexagonally packed (Kasperovich and Hausmann, 2015). Fourthly, due to the large temperature gradients during AM processing, tensile residual stresses typically occur at the surface of the LPBF processed object, leading to a reduced fatigue resistance (Edwards and Ramulu, 2014; Liu et al., 2016; Strantza et al., 2018). Among others, the residual stresses depend on the laser scan strategy, the used raw powder and geometry of the AM processed parts (Parry et al., 2016, 2019). However, according to Leuders et al., the influence of microstructure and residual stresses on the fatigue behavior of LPBF manufactured Ti6Al4V is rather low compared to the porosity (Leuders et al., 2013). Regarding the implants mentioned above, the fatigue strength seems to be sufficient for the stresses occurring in vivo. Regarding higher loaded implants exposed to high bending stresses, such as femoral hip stems, the reduced fatigue resistance of AM processed parts could lead to fatal implant fractures. Implant fractures are traumatic experiences for the affected patients and lead inevitably to revision surgery (Sadoghi et al., 2014). Although fractures of conventional manufactured hip stems are rare, the report of 2022 from the Australian Orthopaedic Association National Joint Replacement Registry showed that 1 % of all revisions in hip arthroplasty is due to breakage of hip stems (Australian Orthopaedic Association, 2022). By implanting hip stems processed by AM having a lower fatigue resistance than wrought material, the number of hip stem fracture related revisions may rise drastically. Therefore, it is important to ensure the product safety of 3D-manufactured highly stressed implants to prevent implant fractures. To gain an optimum fatigue resistance of implants processed by AM, appropriate and effective post-processing, such as thermal and mechanical surface treatments can be applied. The main parameters that can influence the LPBF process and hence can affect the mechanical integrity of the additively manufactured parts are laser power, laser scanning speed, layer thickness and hatch distance (Nguyen et al., 2020). In general, tensile residual stresses, appearing at the surface of the LPBF manufactured Ti6Al4V parts, can be eliminated by appropriate annealing processes (Lin et al., 2021). However, it has been shown that only a hot isostatic pressing (HIP) process is suitable to reduce the porosity inside the material to a minimum (du Plessis and Macdonald E., 2020; Masuo et al., 2018) and, moreover, to reduce the residual stresses that are induced through AM. Furthermore, it was already shown that a heat treatment alone is not sufficient to get similar fatigue values compared to wrought Ti6Al4V specimens due to the remaining porosity (Kasperovich and Hausmann, 2015). After HIP processing, various mechanical surface treatments can be applied to the LPBF manufactured parts, which may improve the fatigue behavior. Thereby, compressive residual stresses can purposefully be induced into the near surface region of AM processed Ti6Al4V specimens, which can further increase the fatigue resistance. A study by Sonntag et al. (2015) already showed an increased fatigue resistance of wrought Ti6Al4V material due to compressive residual stresses that were induced by different mechanical surface treatments such as deep rolling, shot peening and laser shock peening. A study by Kahlin et al. (2020) proved that mechanical surface treatments are also beneficial for the fatigue resistance of LPBF manufactured Ti6Al4V specimens. They reported that the reduction of the surface roughness by the different surface treatments will minimize the notch effect and can therefore contribute to increase the fatigue resistance. In this well conducted study by Kahlin et al., it was also shown, that the compressive residual stresses obviously have a higher impact on the improvement of the fatigue resistance than the reduction of the surface roughness (Kahlin et al., 2020). However, no HIP post-processing was applied in this study to the Ti6Al4V specimens processed by AM in order to reduce the porosity. Instead, a stress relief heat treatment was applied at 730 °C for 2 h under vacuum. In addition, the fatigue behavior of specimens, on which different surface treatments were applied, were compared to as-built specimens, but not to the wrought material using the same test setup. To close this gap of knowledge, the objective of the herein presented study is to further investigate the fatigue behavior of LPBF manufactured Ti6Al4V specimens and to give final answers to the following questions.

1) Is the fatigue resistance of LPBF manufactured Ti6Al4V specimens, receiving a HIP procedure, similar to the fatigue resistance of the wrought material?
2) Is there a requirement to apply an additional HIP process prior to the application of mechanical surface treatments?
3) Which mechanical surface treatment results in a similar fatigue behavior of LPBF manufactured Ti6Al4V specimens as wrought material?
4) Do near surface compressive residual stresses or a reduction of the surface roughness lead to a higher level of fatigue resistance?
5) Does a reduction of the surface roughness after a mechanical surface treatment further increase the fatigue resistance?

2. Materials and methods

In order to answer the five research questions, cylindrical specimens were additively manufactured using LPBF and additionally cylindrical specimens with similar geometry were manufactured from wrought Ti6Al4V material (grade 5). Most of the LPBF manufactured cylindrical specimens underwent a HIP treatment before different surface treatments were applied. A four-point bending setup was used to determine the fatigue strength of the cylindrical samples. In addition, surface roughness testing, X-ray residual stress analyses and metallographic investigations were performed to assess the post-treatment strategies applied.

2.1. Additive manufacturing process and heat treatment

The cylindrical specimens had a diameter of 10 mm, a length of 120 mm and were LPBF manufactured in an upright position without any support structures. The specimens were manufactured using an EOS M 290 system (EOS, Krailling, Germany) and Ti6Al4V Grade 5 powder with a chemical composition in compliance with ISO 5832-3, ASTM F1472 and ASTM F2924 and a powder particle size of 20–80 µm. The process parameters used are presented in Table 1.

To mitigate the process induced residual stresses and to minimize the porosity of the specimens after LPBF manufacturing a HIP process optimized for the alloy Ti6Al4V was applied at a temperature and pressure of 820 °C and 140 MPa, respectively, for 2 h.

Table 1
LPBF processing parameters of the EOS parameter set M 290 Ti64 Grade 5040 V1.

Recoater blade	Nozzle	Inert gas	Sieve	Layer thickness	Min. wall thickness	Volume rate
EOS HSS blade	EOS grid noozle	Argon	90 µm	40 µm	Approx. 0.4 mm	6.2 mm^3/s

2.2. Surface topography treatments

Different mechanical surface treatments were applied to the LPBF cylindrical specimens. The surface treatments were turning, deep rolling, laser shock peening, shot peening and polishing (cf. Fig. 1).

Turning and polishing were applied on six specimens each. The three mechanical surface treatments deep rolling, laser shock peening and shot peening were applied on three specimens with two different intensities (see Table 2).

For the deep rolling process, the hydrostatic tool Ecoroll HG6 (ECOROLL, Celle, Germany) was used and the two applied intensities differ only regarding the used pressure. The laser shock peening was performed according to AMS 2546A and the two intensities differ mainly regarding the applied energy. A dual shoot peening process, consisting of a steel blasting prior to a glass blasting procedure, was applied in two variants. The air pressure of the steel blasting of variant 1 was higher and the peening duration lower compared to variant 2. All post processing methods applied reduced the diameter of the specimen by less than 1 % of the target diameter of 10 mm, hence the effect can be neglected. Only the turning process would lead to a reduction of the diameter of more than 1 %. Therefore, the specimens were printed with a diameter of 12 mm and reduced to a diameter of 10 mm by the turning process. Each diameter of the cylinder specimens was measured before testing using an 838 TA measuring gauge (Mahr, Esslingen, Germany).

2.3. Roughness measurements

The surface roughness of the cylindrical specimens was determined after fatigue testing using a tactile roughness measuring instrument (Perthometer M2, probe NHT 6–100, Mahr, Göttingen, Germany; accuracy: 12 nm). The measurements were carried out (continuously) in axial direction on the cylinder surface at five positions (measuring length: 5.6 mm, limiting wavelength: $\lambda_c = 0.8$ mm). Roughness parameters (R_a – Arithmetic average profile roughness and R_z – Average maximum height of the profile) were determined in accordance with ISO 4287 and ISO 13565. Three samples were used for each surface topography treatment to compare the roughness to the initial state after LPBF-manufacturing. Hence, in total 15 roughness measurements were performed for each group.

Table 2
Process parameters of different surface treatments. DR1 and DR2 = deep rolling variants 1 and 2; LSP1 and LSP2 = laser shock peening variants 1 and 2; SP1 and SP2 = shot peening variants 1 and 2.

	Pressure in bar	Feed in mm	Number of revolutions in U/min
DR1	240	0.032	250
DR2	120	0.032	250

	Energy in J	Pulse width in ns	Call out
LSP1	4.05	18	2.5-18-3
LSP2	5.67	18	3.5-18-3

	Blasting medium	Air pressure in bar	Peening Duration in s	Degree of Coverage in %	Intensity
SP1	Steel 170H	3–3.5	60	200	11–14 A
	Glass AGB12	1–1.5	10–20	125	6 N
SP2	Steel 170H	1.3–1.7	120	200	6–9 A
	Glass AGB12	1–1.5	10–20	125	6 N

2.4. X-ray residual stress analysis

For residual stress analyses in the two principal directions (axial and tangential), a 3-axis X-ray diffractometer in ψ-configuration was chosen and the measurements were performed according to the well-known $\sin^2\psi$ - technique. Ni-filtered Cu Kα-radiation was used to analyze the {213} lattice planes of α/α′-Ti in the 2θ range between 136° and 148° with a step width of 0.1°. Fifteen sample tilts in the range $-60° \leq \psi \leq 60°$ were selected equidistantly distributed over $\sin^2\psi$. A pinhole collimator with a nominal diameter of 1 mm was used as primary aperture, while a symmetrizing aperture according to Wolfstieg with a width of 4 mm was placed in front of the scintillation counter on the secondary side (Wolfstieg, 1976). The data were analyzed using a Pearson VII fit function after the background was subtracted. The diffraction elastic constants (DEC) $E_{\{213\}} = 113$ GPa and $\nu_{\{213\}} = 0.32$ were used for stress calculations. Residual stress depth distributions were determined using electrochemical layer removal in combination with the re-application of X-ray residual stress analysis on the newly generated surfaces for each layer removal step.

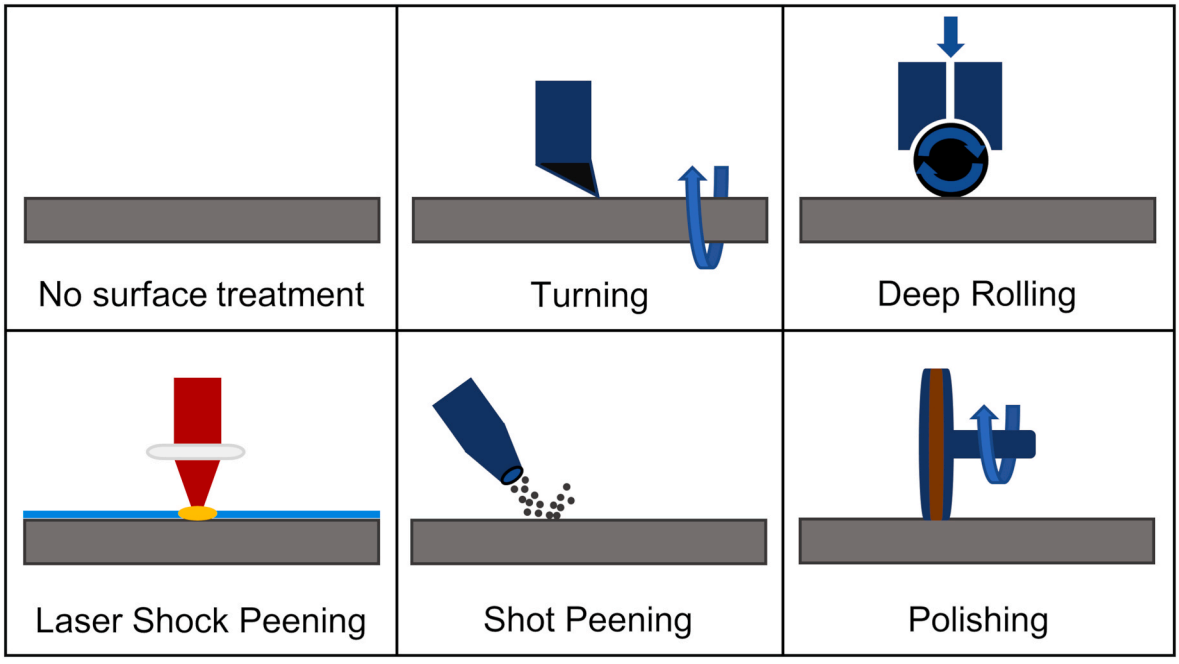

Fig. 1. Different mechanical surface treatments applied to the LPBF manufactured cylindrical specimens.

2.5. Metallography

For metallographic preparation, the LPBF manufactured specimens were cut in longitudinal section and subsequently cold embedded. Silicon carbide papers gradually using smaller grit sizes from P600 to P2500 were used for mechanical polishing. The final polishing was performed using a diamond suspension with a grit size of 9 μm and lubricant followed by etch polishing with 20 ml H_2O_2 and 100 ml oxide polishing suspension (Struers, Willich, Germany). Subsequently, the samples were etched using Weck's reagent. An Axiovert 200 MAT light microscope (Zeiss, Oberkochen, Germany) was used to image the microstructure and a LEO EVO 50 scanning electron microscopy (SEM) (Zeiss, Oberkochen, Germany) was used for reaching higher resolutions. Furthermore, local elemental analysis was performed by means of energy dispersive X-ray spectroscopy (EDS) in the SEM with the aim to check whether a local material transfer was caused by the shot peening process.

2.6. Fatigue testing

For fatigue testing of the cylindrical specimens a four-point bending setup was designed. The cylindrical specimens were placed on two support pins having a diameter of 10 mm, which were 102 mm apart from each other. The two loading pins with 10 mm in diameter had a distance of 34 mm to each other. The relative distance between the support pins and the loading pins were based on ASTM F1264-16. A sinusoidal force at a frequency of 12 Hz was subjected to the specimens. Therefore, the adapter with the two loading pins was fixated at a single-station servo-hydraulic uniaxial test machine (Bosch Rexroth, Lohr am Main, Germany) (Fig. 2A). A Locati-test was used to analyze the fatigue behavior at different load levels (Fig. 2B). In the beginning, 1.0×10^6 cycles with a maximum force of 2.0 kN and a minimum force of 0.1 kN were applied to the cylindrical specimens and in case that breakage occurred, the cycles until failure were recorded. In case the specimens did not fail, the maximum force was increased stepwise by 0.5 kN and for each load level 1.0×10^6 cycles were applied. The minimum force remained constant for each load level at 0.1 kN.

To compare the different test groups the cycles to failure were calculated according to the procedure applied in Sonntag et al. using the following equation (Sonntag et al., 2019):

$$F_D = F_{-1} + 500N \times \frac{NCY}{10^6}$$

In this equation, F_{-1} is the maximum force in the load interval before failure and NCY is the number of cycles to failure in the respective interval.

Exemplary samples were used after the fatigue tests to look for subsurface failure origins using a digital microscope (VHX-5000, Keyence, Japan).

2.7. Objectives of the research project

The research project should answer the following questions:

Research question 1: The fatigue resistance of 6 LPBF processed Ti6Al4V specimens receiving a HIP procedure but no surface treatment and the fatigue resistance of 6 wrought Ti6Al4V alloy specimens were compared. Thus, the results will indicate if a HIP treatment of LPBF manufactured Ti6Al4V without any additional mechanical surface treatment is sufficient to get similar fatigue results as for the conventional wrought material.

Research question 2: The fatigue resistance of 6 LPBF manufactured Ti6Al4V specimens receiving a HIP procedure and subsequently a turning process were compared to the fatigue resistance of 6 LPBF processed Ti6Al4V specimens receiving no HIP procedure but the same turning process. Thus, the results will indicate whether a HIP treatment is necessary prior to applying a mechanical surface treatment.

Research question 3: The influence of deep rolling, laser shock peening, shot peening and polishing after HIP processing of LPBF manufactured Ti6Al4V specimens on the fatigue behavior were analyzed. For each mechanical surface treatment, except for the polishing process, two different intensities were used for three specimens each. For the polishing process, 6 specimens were treated equally. Thus, the fatigue resistance of the surface treatments subsequent to the HIP process can be compared to the fatigue resistance of the wrought material.

Research question 4: It is expected that the polishing process should lead to the lowest compressive residual stresses close to the surface and the lowest surface roughness compared to the other mechanical surface treatments. Therefore, the fatigue results indicate, whether the process induced compressive residual stresses or the reduction of the surface roughness has a major impact on the fatigue resistance.

Research question 5: To investigate, whether a combination of a mechanical surface treatment inducing characteristic residual stresses in the near surface region and a mechanical surface treatment leading to a low surface roughness will further increase the fatigue resistance compared to a single surface treatment, shot peening and polishing were combined. Therefore, 12 LPBF manufactured Ti6Al4V specimens received a HIP-procedure and afterwards 6 specimens moreover received a polishing process prior to the shot peening process, and 6

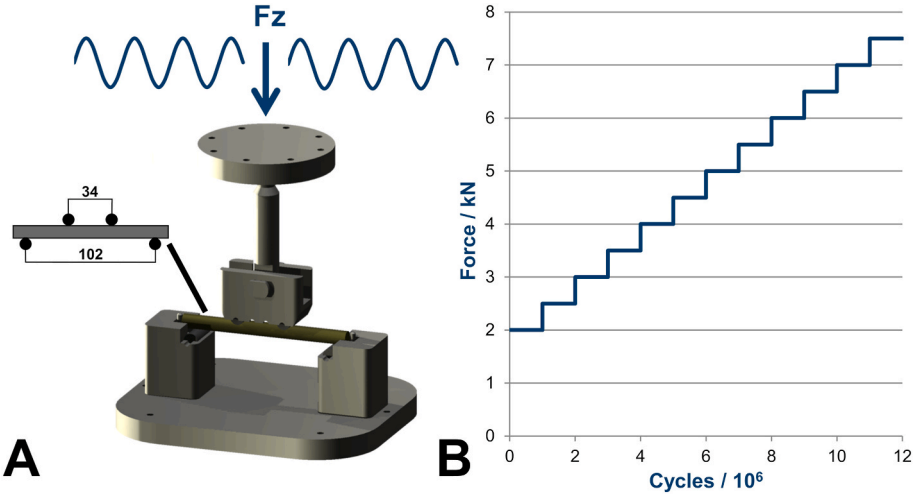

Fig. 2. Illustration of the four-point bending setup for cyclic testing of the cylindrical specimens including the distances of the inner and outer rollers in mm (A). Locati-test scheme to analyze the fatigue behavior at increasing maximum load levels (B).

specimens received the same two mechanical surface treatments, but in reverse order. The fatigue results of the combined surface treatments were compared to the fatigue results of the single surface treatments.

2.8. Statistical analysis

Mean and standard deviations of all fatigue results were calculated. To compare the fatigue test results non-parametric analyses were used (Kruskall-Wallis-test and Mann-Whitney-U-test) due to the small number of specimens. A p-value of ≤ 0.05 was considered being significant. All statistical calculations were carried out using the statistical evaluation software SPSS 28 (IBM, Amonk, NY, USA).

3. Results

3.1. Roughness measurements

The mean surface roughness R_a and R_z of the LPBF manufactured Ti6Al4V specimens after the HIP process, but without any additional mechanical surface treatment, were 9.55 µm ± 1.04 µm and 48.14 µm ± 5.93 µm, respectively. The surface roughnesses after the different surface treatments are shown in Table 3.

In general, all applied mechanical surface treatments led to a reduction of the surface roughness compared to the as built parts in the condition subsequent to the HIP process (see Table 3). Thereby, the higher pressure of 240 bar applied during variant DR1 led to a reduced surface roughness compared to DR2 receiving only 120 bar. For the LSP2 process variant a higher energy was used, which led to a lower surface roughness compared to the variant LSP1. At least, the higher air pressure of 3–3.5 bar of variant SP1 led to a reduced surface roughness compared to SP2 receiving only 1.3–1.7 bar. Polishing led to the smallest surface roughness. The roughness of a polishing process after the SP1 process led to a similar roughness as polishing alone. The roughness of a SP1 process after a polishing process led to a similar roughness as a SP1 process alone. As shown in Table 3, the surface roughness strongly depends on the applied mechanical surface treatment and visible differences regarding the surface topography can be found (cf. Fig. 3).

3.2. X-ray residual stress analysis

The results of X-ray stress analyses are presented as follows: First, the results for the LPBF processing followed by HIP processing are compared with the results after subsequent turning of the surface (cf. Fig. 4). In Fig. 5 the results of the mechanical surface treatments deep rolling, laser shock peening and shot peening are directly compared to each other. The results of the polishing process are separately presented in Fig. 6. In Figs. 4–6 always the residual stress depth distributions and the depth distributions of the average integral width $\overline{IW}$ of the $\alpha_{\{213\}}$ diffraction lines are shown. The values of the $\overline{IW}$ in this comparative study, i.e. by always applying the identical measuring conditions and parameters, can be used in a qualitative way to assess the amount of cold working (work hardening) induced by the different processing or treatment variants, respectively. Lattice defects induced through plastic deformation by means of mechanical surface treatments cause a broadening of the X-ray diffraction lines, hence, it is expected that this so-called peak broadening, which can be expressed by the $\overline{IW}$, scales with the degree of cold working induced by the mechanical post-treatments.

3.2.1. Residual stress depth distributions

First, only the residual stress depth distributions are described. While the specimen after LPBF plus HIP (Fig. 4) show no significant residual stress in both measurement directions at the surface, and can technically be considered as being stress-free, the value for the turned specimens starts at about −469 MPa and reaches the zero residual stress level at a depth of about 155 µm, i.e. the turning process results in a residual stress depth distribution with a relatively small depth range. The two measurement directions do not differ much with respect to their residual stress depth distributions.

The residual stress depth distributions of the surface treatments deep rolling (DR1 and DR2), laser shock peening (LSP1 and LSP2) and shot peening (SP1 and SP2) are shown in detail in Fig. 5.

As stated before, for each of these three surface treatments, two different parameter variants were investigated. Unexpectedly, for the process parameters chosen here, laser shock peening resulted in tensile residual stress in the near surface region with the highest values determined close to the surface. For the post-treatment variant LSP1, the maximum values of about 322 MPa and 222 MPa are slightly higher than those determined for variant LSP2 with about 81 MPa and 115 MPa in axial and tangential direction, respectively. At a depth of about 72 µm, the tensile residual stress state changes to the compressive range and shows peak values of about −216 MPa and −265 MPa in axial and tangential direction, respectively. The deep rolled state with the rolling pressure of 240 bar (DR1) shows maximum compressive residual stress in axial direction with a value of about −1046 MPa at a depth of about 30 µm, whereas in tangential direction the maximum residual stress of −727 MPa occur at a depth of about 222 µm. The value directly at the surface is about −178 MPa in tangential direction and about −581 MPa in axial direction. At a rolling pressure of 120 bar (DR2), the surface values show a comparable value with about −256 MPa for the tangential direction and −298 MPa in axial direction. The results clearly indicate that, as expected, higher rolling pressures result in higher maximum compressive residual stress and a greater depth range. Moreover, in particular for the higher rolling pressure it can be noticed that the residual stresses generated during deep rolling are strongly directional dependent. This is not the case with shot peening. Here, no differences in the residual stress distributions between axial and tangential direction can be noticed. For this reason, only one direction is considered in the following. The shot peened specimens with parameter set SP1 have slightly higher compressive residual stresses than specimens processed with parameter set SP2. While the surface value for variant SP1 is approx. −940 MPa, the value for variant SP2 is only about −790 MPa. In both cases, the maximum value is at a depth of about 24 µm with about −947 MPa and −894 MPa for variants SP1 and SP2, respectively. The range of the depth distribution with about 306 µm for variant SP1 is about 100 µm higher than for variant SP2.

Fig. 6 shows the results of the residual stress analyses for the polished surfaces – in (a) for pure polishing and for polishing before (b) or after (c) shot peening using the more intense shot peening variant SP1.

Table 3
Surface roughness Ra and Rz after the application of different mechanical surface treatments to the LPBF manufactured and HIP treated specimens. T = turning, DR = deep rolling, LSP = laser shock peening and SP = shot peening, P = polishing. The numbers assigned to the process (1,2) indicate the parameter set of the mechanical surface treatment (see Table 2).

Surface Treatment	T	DR1	DR2	LSP1	LSP2	SP1	SP2	P	SP1+P	P + SP1
R_a in µm	0.66 ± 0.12	1.24 ± 0.29	2.48 ± 0.85	6.10 ± 0.76	4.22 ± 1.13	3.17 ± 0.47	3.61 ± 0.56	0.16 ± 0.07	0.16 ± 0.04	3.29 ± 0.37
R_z in µm	3.22 ± 0.46	10.93 ± 2.02	16.53 ± 3.28	29.19 ± 3.69	20.37 ± 3.97	15.55 ± 2.36	18.31 ± 3.22	1.71 ± 1.00	1.44 ± 0.44	15.91 ± 1.85

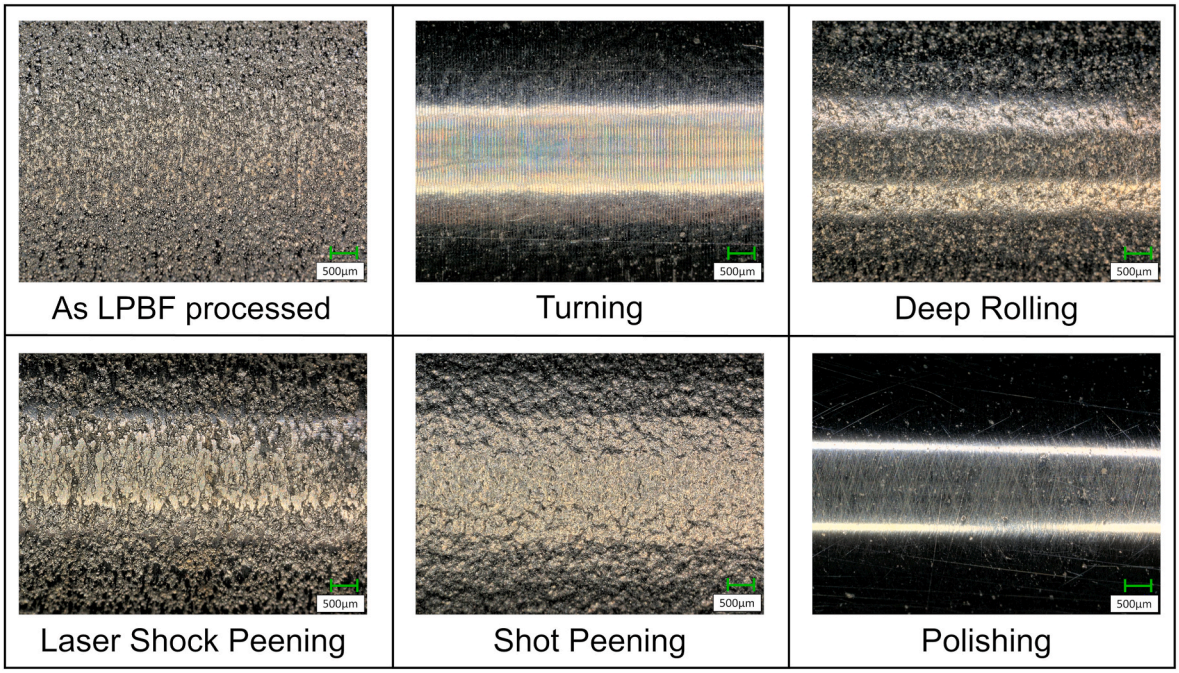

Fig. 3. Surface topographies after application of different surface treatments recorded by means of light optical microscopy (digital microscope Keyence VHX-5000).

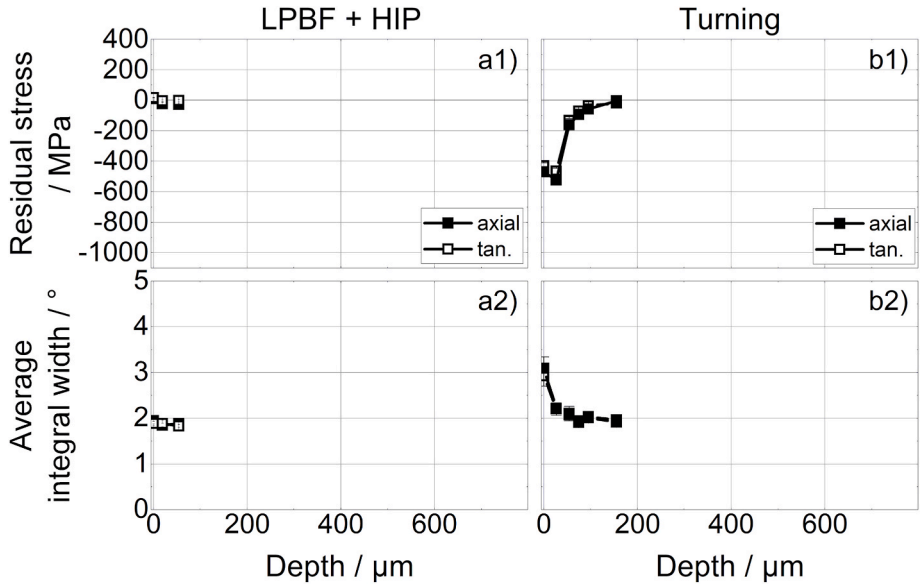

Fig. 4. Residual stress depth distributions and depth distributions of the average integral width of the X-ray diffraction lines after LPBF and HIP processing (left, a) and after LPBF, HIP processing and subsequent turning (right, b).

First, it can be noticed that polishing does not lead to a directional dependence of the residual stress distributions. For the polished specimen the compressive residual stress value at the surface starts at about −298 MPa and drops to a zero level of residual stresses already at a depth of approx. 24 µm, hence, the depth range of the region affected by the polishing process is comparably shallow. In addition to the polishing treatment of the LPBF surface (Fig. 6a), additional shot peening of the surface was carried out subsequent (Fig. 6b) or prior (Fig. 6c) to polishing. In both cases, this resulted in significantly higher levels of compressive residual stresses with a much higher depth range. These amount to about −800 MPa in each case and again show no directional dependence. The two variants also differ only minimally in their depth range, while the depth range is furthermore comparable to that one of the shot peening treatments using process parameter set SP1 alone (cf. Fig. 5).

3.2.2. *Average integral width ($\overline{IW}$)*

In the following, the $\overline{IW}$ of the X-ray diffraction lines are considered, for which the depth distributions in Figs. 4–6 are displayed in the lower row of the images. As expected, the average $\overline{IW}$ shows no directional dependence in either measurement direction under any machining condition. For the state after LPBF and HIP processing (Fig. 4a2), the average $\overline{IW}$ remains constant at a value of about 1.885°, which is considered as reference. The difference to this reference should be used for discussing the effect of the different mechanical surface treatments. For the turning state (cf. Fig. 4b2), an average $\overline{IW}$ of about 2.822° was

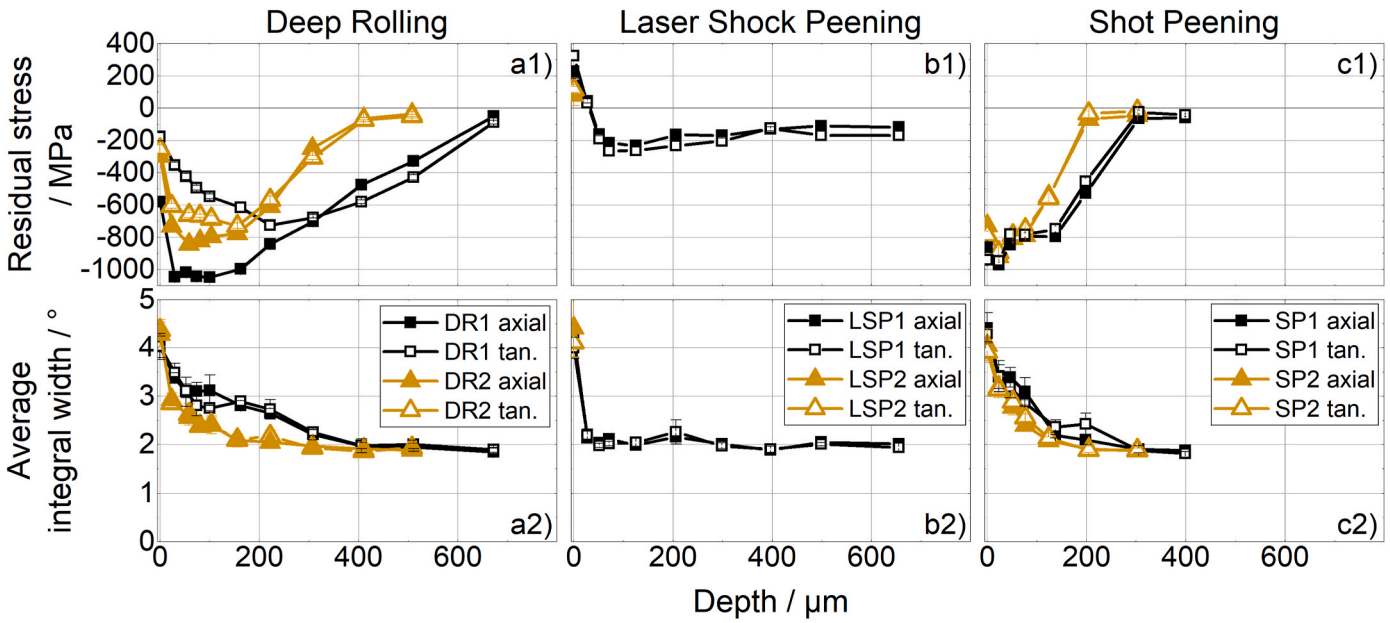

Fig. 5. Residual stress depth distributions and depth distributions of the average integral width of the X-ray diffraction lines after deep rolling with the variants DR1 and DR2 (a), laser shock peening with the variants LSP1 and LSP2 (b), and shot peening with the variants SP1 and SP2 (c).

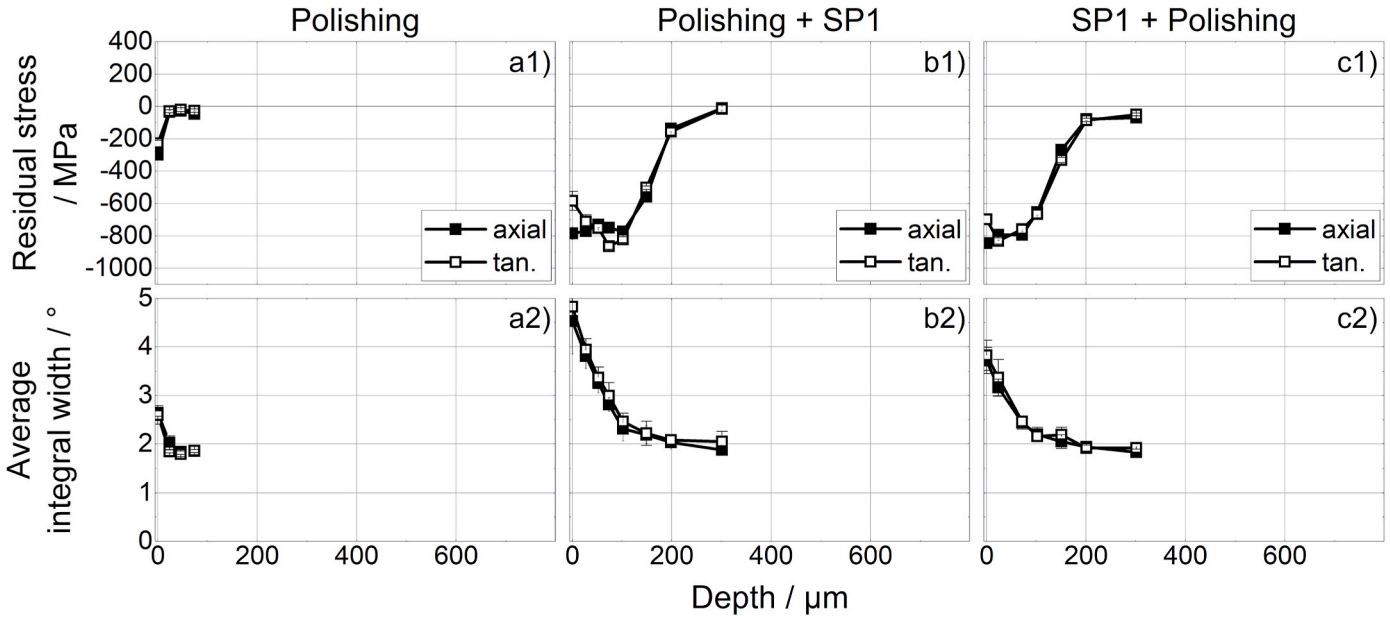

Fig. 6. Residual stress depth distributions and depth distributions of the average integral width of the X-ray diffraction lines after polishing (a), polishing before shot peening (b) and polishing subsequent to shot peening (c) of the LPBF manufactured specimens, that received a previous HIP process. In both cases (b and c) with the shot peening process parameter set SP1.

determined, which drops down to a value of only about 1.910° at a depth of about 75 µm. The $\overline{IW}$ is a rather sensitive value to discuss the depth range of the mechanical surface treatment. Hence, since in a depth of approx. 75 µm the reference $\overline{IW}$ value is almost reached, this marks the approximate depth range of the turning process. Laser shock peening (cf. Fig. 5b2) results in a comparable high average $\overline{IW}$ of about 3.995° at the surface for both variants. For the variant LSP1, the $\overline{IW}$ value drops to about 1.981° at a depth of approx. 52 µm and remains at this low level. Hence, it can be concluded that the layer affected by plastic deformation through work hardening is only limited to the first 50 µm. Compared to laser shock peening, the average $\overline{IW}$ at the surface of the deep-rolled specimens (cf. Fig. 5a2) differs slightly between the two parameter sets. The difference is about 0.343°, the higher value of approx. 4.368° in maximum being due to the variant DR1, which indicated that the more intense deep rolling condition (higher rolling pressure) results in the slightly higher $\overline{IW}$ values. The $\overline{IW}$ value drops to 1.864° at a depth of approx. 411 µm. In comparison, for the variant DR2 the $\overline{IW}$ value drops from about 4.025° in maximum to a value of about 1.977°, i.e. close to the reference value, at a comparable depth of approx. 406 µm. This means that the depth range of the deep rolling is much higher in comparison to turning and laser shock peening. For the shot peened specimen (cf. Fig. 5c2), the average $\overline{IW}$ of about 4.410° in maximum for the variant SP1 is higher than the respective value of about 4.046° for the variant SP2. Within a depth of approx. 306 µm for the variants SP1 and

205 μm for SP2, respectively, both values decrease to a value of about 1.900°. This means at first that the degree of work hardening induced by shot peening is in the same range as for the deep rolling process and that moreover the depth region affected by shot peening is slightly lower in comparison to the deep-rolling treatment.

For the polished specimen (cf. Fig. 6a2) $\overline{IW}$ values of about 2.597° were determined under identical measuring conditions, which drop down to a value of 1.847° close to the reference within the first 24 μm. If shot peening is applied subsequent to polishing (cf. Fig. 6b2), the average $\overline{IW}$ increases significantly to a value of about 4.825°, which is slightly above the value of the purely shot peened variant (cf. Fig. 5c2). Within a depth range of approx. 200 μm, this value decreases to about 2.079°. If, on the other hand, shot peening is performed prior to polishing (Fig. 6c2), the average $\overline{IW}$ at the surface is only 3.822°, which also falls to 1.913° after a depth of about 201 μm.

3.3. Metallography

Fig. 7a shows a light optical microscopy image of the cross-sectional view of the near-surface structure of the materials state after LPBF manufacturing and subsequent HIP treatment, while Fig. 7b shows an SEM image in back scattered electron (BSE) contrast from the bulk of the specimen of the same materials state. Fig. 7a indicates that the manufacturing process results in a rather high surface roughness (cf. Table 3). The SEM image (cf. Fig. 7b) shows the bulk microstructure of the samples at a much higher resolution. The grain orientation contrast from BSE imaging indicates a lamellar microstructure, whereby the lamellae represent the hexagonal α-Ti phase and the bright areas between the lamellae can be assigned to the b.c.c. solidified β-Ti phase. The brighter appearance in the BSE contrast is due to the material contrast since the cubic β-phase exhibit the slightly higher effective atomic number Z.

Fig. 8 presents micrographs of metallographically prepared and etched longitudinal-sections of the specimens recorded by means of light optical microscopy to allow for a comparison of the near-surface microstructure between deep rolled, laser shock peened and shot peened surfaces. While laser shock peening produces a rather rough surface, the other two mechanical surface treatments deep rolling and shot peening result in a significantly smoother surface. Nevertheless, minor defects such as small microcracks and isolated furrows are visible in both surfaces after deep rolling and after shot peening. These extend into the material up to a maximum of about 20 μm.

Finally, Fig. 9 presents corresponding light optical microscopy images for the polished surface states. In Fig. 9a the purely polished state is shown, whereas in Fig. 9b the state after polishing followed by an additional shot peening treatment is shown. In Fig. 9c, on the other hand, shot peening was applied subsequent to polishing. Although, shot peening after polishing led to a higher surface roughness than polishing after shot peening or polishing alone (cf. Table 3), the images indicate that the surfaces of the three cases are comparatively smooth. Shot peening after polishing resulted in occasional irregularities, which however, are much less compared to shot peening without polishing. If polishing is performed subsequent to shot peening, such moderate surface elevations are no longer visible. However, the furrows and microcracks being present after shot peening could not be completely removed, so that - according to the images - isolated defects can also be found for these states, however, at much lower magnitudes in comparison to the purely shot peened state (cf. Fig. 8c).

3.4. Fatigue testing

In a first analysis, the fatigue resistance of the wrought Ti6Al4V material was compared to the LPBF manufactured specimens after subsequent HIP processing (cf. Fig. 10).

The wrought material showed a significant higher estimated load to failure (6.07 ± 0.54 kN) compared to the LPBF manufactured specimens directly after HIP processing, i.e. without further mechanical surface treatment. LPBF plus HIP-processed specimens exhibit an estimated load to failure of only about 2.02 ± 0.16 kN ($p = 0.002$). The failure origins of the exemplary samples (wrought Ti6Al4V and LPBF manufactured Ti6Al4V receiving a HIP-process) occurred at the surface, where the highest tensile stress acts.

In a second analysis series, the effect of a HIP process in combination with a surface treatment on the fatigue resistance of LPBF manufactured specimens was evaluated (Fig. 11).

Thereby, the HIP procedure in combination with a turning process led to a significant higher estimated load to failure (6.22 ± 0.42 kN) than a turning process of the LPBF manufactured Ti6Al4V specimens without any HIP procedure having an estimated load to failure of 3.64 ± 0.37 kN ($p = 0.002$).

Beside the turning process, four different mechanical surface treatments (deep rolling, laser shock peening, shot peening and polishing) were evaluated in combination with the same HIP procedure. In Fig. 12, the fatigue behavior of these different mechanical surface treatments of the LPBF manufactured Ti6Al4V specimens after the subsequent HIP process were compared to the fatigue behavior of the wrought Ti6Al4V material.

For deep rolling, laser shock peening and shot peening, the fatigue test results of both process parameter sets applied (three specimens were tested each) were combined for the comparison to the standard wrought material. The results could be combined, because no significant difference in fatigue strength between the two intensities could be found for

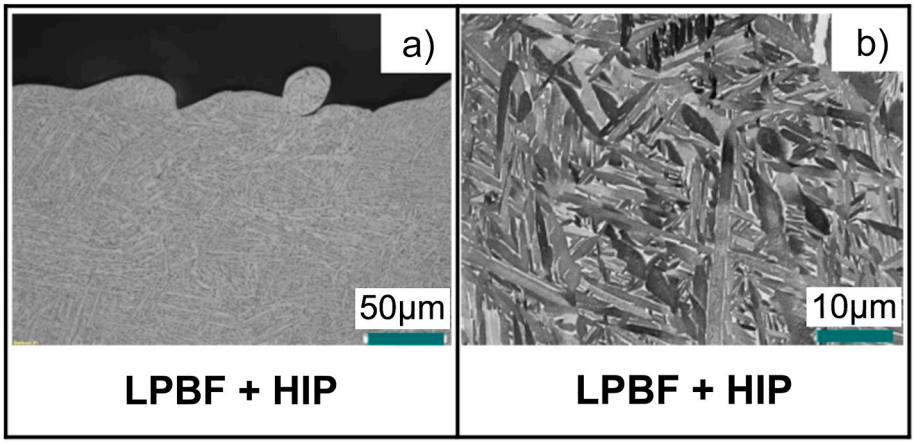

Fig. 7. Light optical microscopy image of the state after LPBF manufacturing and subsequent HIP treatment close to the sample surface a) and SEM image (back scattered electron (BSE) contrast) at higher magnification b) for the same sample state recorded in the bulk of the samples (cross sectional view).

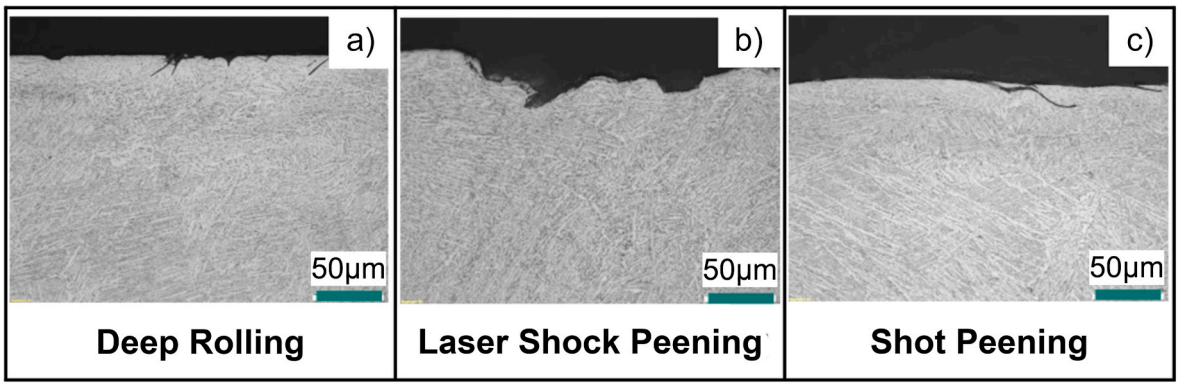

Fig. 8. Light optical microscopy images after deep rolling (DR1 = a), laser shock peening (LSP2 = b) and shot peening (SP1 = c).

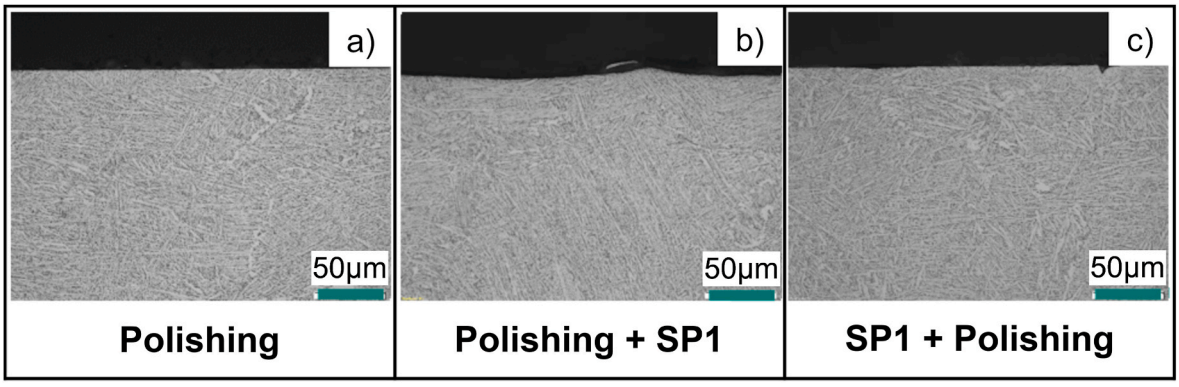

Fig. 9. Light optical microscopy images after polishing (a) and polishing prior to (b) and subsequent to (c) shot peening (SP1).

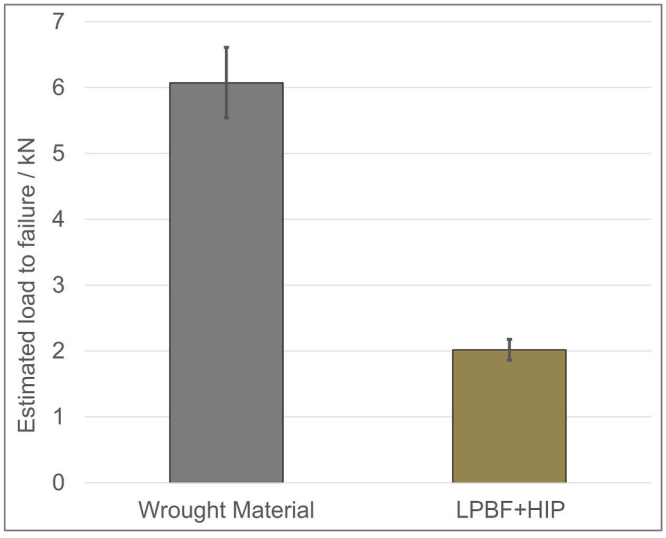

Fig. 10. Estimated load to failure of wrought Ti6Al4V material (n = 6) vs. LPBF manufactured Ti6AL4V material (n = 6) after subsequent HIP-treatment.

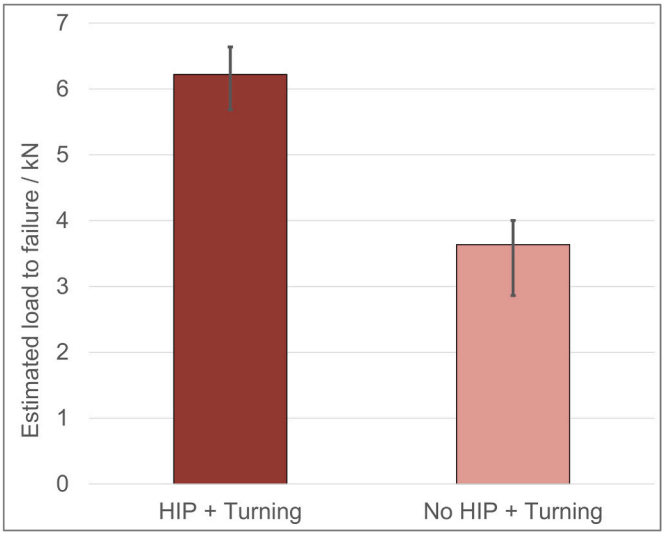

Fig. 11. Estimated load to failure of LPBF manufactured Ti6Al4V material including a turning process with (n = 6) and without (n = 6) previous HIP treatment.

the deep rolling ($p = 0.100$), the laser shock peening ($p = 0.100$) and the shot peening ($p > 0.99$) treatments. No significant differences could be found between the estimated load to failure of the wrought material (6.07 ± 0.54 kN) and the estimated load to failure of the mechanical surface treatments turning (6.22 ± 0.42 kN), deep rolling (5.76 ± 0.39 kN) and shot peening (5.68 ± 0.34 kN) ($p > 0.99$). The mechanical surface treatments laser shock peening (2.20 ± 0.33 kN) and polishing (2.58 ± 0.30 kN) showed a significantly lower fatigue resistance compared to the wrought material ($p \leq 0.015$). Sub-surface failure origins could be found for the mechanical surface treatments turning, deep rolling and shot peening, which induced high compressive residual stresses at the specimens surface. A sub-surface failure is shown in Fig. 13 for a deep rolled specimen.

In an additional analysis, the fatigue resistance of two combined mechanical surface treatments (shot peening and polishing) were

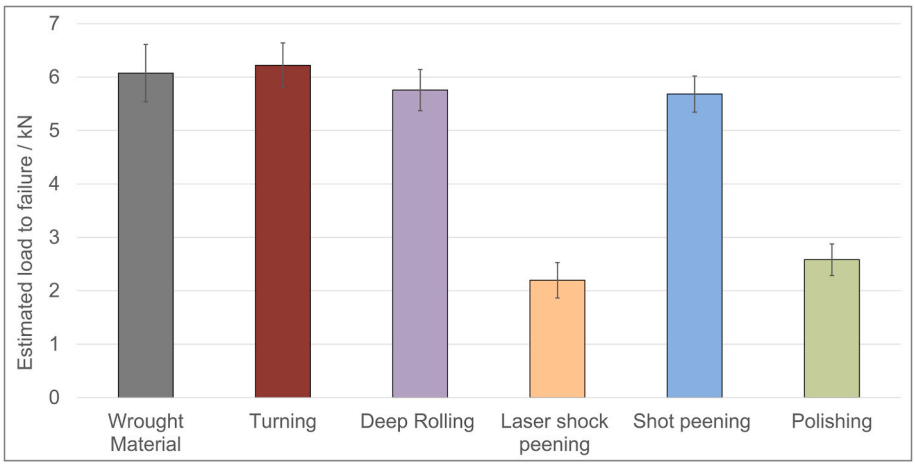

Fig. 12. Estimated load to failure of different mechanical surface treatments applied to LPBF manufactured Ti6Al4V specimens after subsequent HIP treatment in comparison with the wrought Ti6Al4V material (n = 6 for each group).

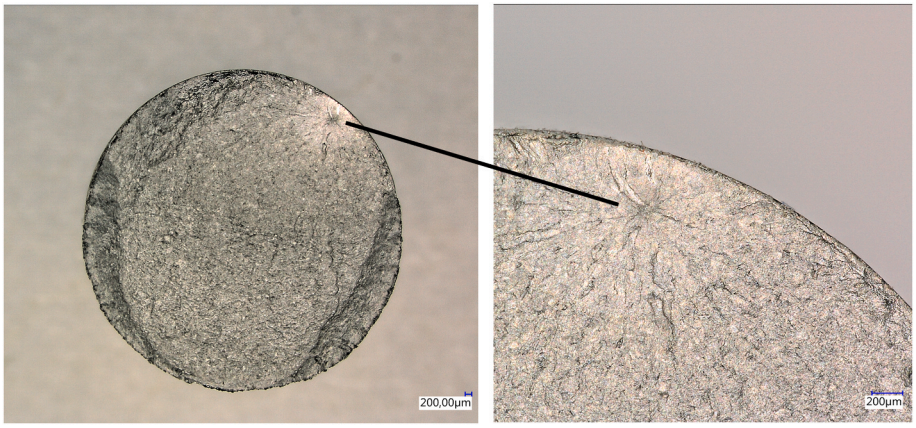

Fig. 13. Sub-surface failure origin of a deep rolled specimen after fatigue testing (whole fracture surface = left and failure origin in detail = right).

compared to the single mechanical surface treatments (Fig. 14).

Polishing alone showed a significantly lower estimated load to failure of 2.58 ± 0.30 kN compared to shot peening alone (5.68 ± 0.34 kN) ($p = 0.001$). The polishing subsequent to shot peening led to an estimated load to failure of about 5.40 ± 0.22 kN. The polishing prior to shot peening led to an estimated load to failure of about 5.33 ± 0.39 kN. No difference between shot peening and the combination of shot peening and polishing was found regarding the estimated load to failure ($p > 0.99$). The fatigue resistance of the combined surface treatment was not affected by the order of the applied single treatments ($p > 0.99$).

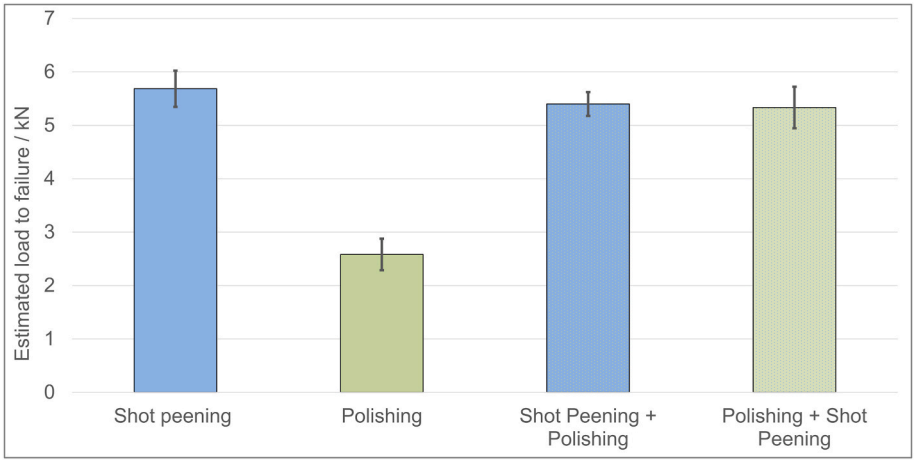

Fig. 14. Estimated load to failure of a combination between shot peening and a polishing procedure to the single surface treatments applied to LPBF manufactured specimens after subsequent HIP treatment (n = 6 for each group).

4. Discussion

In the current study the influence of a HIP procedure and different surface treatments on the fatigue behavior of LPBF manufactured cylindrical specimens were analyzed. Thereby, the impact of residual stresses, the microstructure and the surface roughness on the fatigue resistance was investigated. The overall objective was to find a suitable process chain to manufacture hip implants individually tailored to the patient using LPBF without sacrificing patient safety, i.e. it should be ensured that the additively manufactured implants have the same failure capability after an appropriate post treatment as conventionally manufactured components. In addition, sufficient surface roughnesses should be achieved by the surface treatments, which could be applied on the shaft area (rough) and on the neck area (smooth). In the current study, a cyclic four-point bending setup was used to evaluate the fatigue behaviors of the tested groups. This test setup was chosen because bending is the most dominant loading for hip implants and may lead to dramatic implant fractures. In contrast, in the current literature on LPBF manufactured specimens typically cyclic tensile tests are used to evaluate the fatigue resistance of different post-treatments (Kasperovich and Hausmann, 2015; Shui et al., 2017; Wycisk et al., 2013; Xu et al., 2022).

The comparison between conventionally manufactured Ti6Al4V and LPBF manufactured Ti6Al4V receiving only a HIP treatment, but no further mechanical surface treatment revealed a more than threefold decrease of the fatigue resistance for the specimens processed by AM. A turning process alone as surface treatment without a previous HIP process led to approximately half of the fatigue resistance compared to specimens receiving a HIP treatment prior to a turning process. Only when applying a HIP treatment in combination with a suitable surface treatment similar fatigue results were found as for the wrought material, i.e. for the specimens that were produced following the conventional manufacturing route. Thereby, a HIP treatment in combination with mechanical surface treatments as turning, deep rolling or shot peening were promising. Polishing and laser shock peening showed less than half as low fatigue results than the wrought Ti6Al4V material.

In general, the strength and hardness of Ti6Al4V specimens produced by AM is comparable to traditional manufacturing methods like casting or milling but leads to a reduced ductility and fatigue performance, due to keyholes, gas pockets and unmelted particles (Liu et al., 2023; Qiu et al., 2013). A HIP treatment typically leads to a reduction in strength compared to the as build parts, but is effective to close nearly all lack-of-fusion porosity, except of interconnected pores and pores near the surface (Benzing et al., 2019; du Plessis and Macdonald E., 2020; Snow et al., 2023). Residual stress analyses in this study showed that the HIP treatment led to a residual stress relief to a minimum for the LPBF manufactured specimens, which was to be expected. Tensile residual stresses, which may have originated from different cooling rates during the manufacturing process and may have a detrimental impact on the fatigue behavior, were eliminated by the applied HIP treatment. However, the mitigation of residual stresses induced and the reduction of porosity were not sufficient to get similar fatigue resistance as for the wrought Ti6Al4V material. This may be mainly due to the rather high surface roughness that remained and the typical lamellar martensitic microstructure of the specimens processed by AM. In the current literature a HIP process of LPBF manufactured specimens typically led to an increased fatigue resistance compared to as built parts (Jurg et al., 2022; Mertova et al., 2018; Xu et al., 2022; Zhao et al., 2016). However, different fatigue results (130 MPa–550 MPa) between these previous studies exist, which may be influenced by different processing parameters and the resulting microstructures and surface roughnesses of specimens as well as different HIP treatments and test conditions (Nguyen et al., 2020; Pegues et al., 2018).

The results of the present study further showed that a reduction of the surface roughness and the compressive residual stresses close to the surface have a relatively small effect on the fatigue resistance, if the porosity of the AM Ti6Al4V was not reduced to a minimum by a previous HIP treatment. The specimens receiving the HIP and turning procedure typically failed at nearly the same load level as the wrought material. The fatigue resistance of the specimens receiving a turning process, but no HIP treatment was approximately half of that. Alegre et al. applied a fatigue test on LPBF manufactured specimens receiving a machining process after a HIP procedure and compared the results to other literature performing the same procedure and to wrought material (Alegre et al., 2022). The results agree with the results of the herein presented study that machined LPBF/Ti6Al4V specimens, receiving a previous HIP procedure, have a comparable fatigue resistance as specimens manufactured using wrought material. Kasperovich and Hausmann tested machined LPBF/Ti6Al4V specimens with and without a previous HIP treatment using a fatigue tensile test at a maximum stress of 600 MPa ($R = -1$) (Kasperovich and Hausmann, 2015). The machined specimens with previous HIP treatment survived between 140,000 and 380,000 cycles and the machined specimens without HIP treatment only between 10,000 and 30,000 cycles, respectively. Mertova et al. compared machined Ti6Al4V samples with and without previous HIP treatment and found an approximately 1.5 fold increase of the fatigue limit, when applying a previous HIP treatment (Mertova et al., 2018). The results of this study and previous literature indicate that the combination of a HIP-treatment and a post surface treatment is necessary for LPBF manufactured hip stems to be safe for the patient.

Deep rolling and shot peening in combination with a HIP treatment led to similar fatigue results as a combination of HIP treatment and a turning process or the wrought Ti6Al4V material itself. This may be due to the high compressive residual stresses as well as the comparably low surface roughness. The maximum compressive residual stresses of the shot peening processes were comparable to the deep rolling processes and higher compared to the turning process. However, on the one side the depth ranges of the shot peening processes were higher than for the turning process but on the other side lower than for the deep rolling processes. The exemplary analyses of the failure origins showed, that sub-surface failures occurred for deep rolling, shot peening and turning, which implies a high fatigue resistance at the specimens surface. In the present study, the surface roughness of the shot peening process was higher compared to the turning and deep rolling process, but by far lower than the LPBF manufactured specimens that did not receive any surface treatment. However, the amount and depth range of the compressive residual stresses as well as the surface roughness clearly depend on the applied process parameters.

Deep rolling of conventionally manufactured Ti6Al4V specimens leads to an increased fatigue resistance compared to untreated Ti6Al4V specimens (Altenberger et al., 2012; Sonntag et al., 2015). Due to the increase in compressive residual stresses close to the surface with the highest depth range (compared to the other mechanical post-treatments) and the reduction of the surface roughness ($R_a < 2.5$ µm), the deep rolling process in the current study led to high fatigue results, which were comparable to wrought material. However, the residual stress distributions for the tangential and the axial components showed the highest differences compared to the other surface treatments indicating a distinct directional dependence of the in-plane residual stress distribution. This can be expected and can be explained by the Hertzian contact theory between two rounded specimens in combination with the process sequence, i.e. by taking into account the deep rolling direction (Hertz, 1882).

Wycisk et al. found a 15 % lower fatigue limit of the shot peened LPBF manufactured Ti6Al4V specimens compared to wrought material. However, only a stress-relieve of 650 °C for 3 h was performed, instead of a HIP treatment. A study by Bendetti et al. compared stress relieved Ti6Al4V specimens receiving a subsequent shot peening procedure with specimens receiving only a HIP treatment (Benedetti et al., 2017). The shot peened specimens showed a superior fatigue limit in monotonic tensile tests on cylindrical hourglass specimens after 5×10^6 cycles, but the fatigue limit was reduced by approximately 30 % for high cycle fatigue testing (50×10^6 cycles), which was lower than the fatigue

resistance after 50 × 10^6 cycles of specimens receiving a HIP process. This result justifies the approach of this study to perform a combination of HIP and surface treatment as shown in Fig. 12.

Polishing or laser shock peening led, in the current case, to lower fatigue test results for cyclic four-point-bending than turning, deep rolling and shot peening.

For the polishing process alone, the lowest surface roughness was observed, but the compressive residual stresses were relatively low. This indicates that, in the present case, the compressive residual stresses have a higher impact on the fatigue resistance than the reduction of the surface roughness. Kahlin et al. also reported a relatively low influence of surface roughness on the fatigue resistance compared to compressive residual stresses (Kahlin et al., 2020). However, they used cyclic tensile tests instead of four-point bending tests.

The laser shock peening with the process parameters listed in Table 2 led to tensile residual stress depth distributions in the near surface region, changing to compressive residual stresses after a depth of approximately 72 μm. In addition, the laser shock peening reduced the surface roughness compared to the LPBF manufactured specimens after the HIP treatment, but the surface roughness was highest compared to the other mechanical surface treatments considered here. Both parameters let to a fatigue resistance of laser shock peened specimens, which was only slightly higher than the fatigue resistance of the specimen without any surface treatment. A study by Jiang et al. found even lower fatigue resistances for laser shock peened LPBF/Ti6Al4V specimens compared to the as built parts and heat-treated specimens (955 °C in vacuum for 2 h) (Jiang et al., 2021). The authors explained this finding with inherent defects, an increased surface roughness and non-uniform residual stresses. Although, near-surface compressive residual stresses were found for the laser shock peened specimens, tensile residual stresses were found for the first measuring point (closest measuring point to the surface), which shows similarities to the current study (Jiang et al., 2021). From this it can be concluded, that laser shock peening must be assessed as critical, i.e. the choice of suitable laser shock peened parameters is obviously very sensitive. This means on the other side that for LPBF manufactured hip stems, this technique might be too risky, because of tensile residual stresses that can occur at the implants surface, with respect to the applied laser shock peening parameters.

Kumar et al. expressed the thesis that shot peening and its ability to introduce compressive residual stresses and closing pores near the surface is mainly suitable under rotating bending fatigue conditions (Kumar and Ramamurty, 2020). Hip stems typically are subject to alternating bending stress under in vivo conditions. Similar to rotating bending stress, alternating bending stress leads to the highest stress at the specimen surface. Therefore, shot peening may also be a suitable procedure for hip implants. In addition, for parts having a simple geometry, where uniaxial loads are acting, a deep rolling or machining process like turning may be sufficient. However, for complex shaped parts like hip stems, a shot peening process may be the more appropriate variant, especially due to the equi-biaxial compressive residual stresses in tangential and axial direction and not least since shot peening can be better adapted to complex components' geometries in comparison to e.g. deep rolling, provided that the surface is accessible for the peeing process.

The combination of shot peening and polishing did not lead to an increased fatigue resistance regardless of the sequence (shot peening prior or subsequent to polishing). However, the combination of both surface treatments did not lead to a reduced fatigue resistance, too. The combination shot peening before polishing may have different applications, when high fatigue strengths and a smooth surface are necessary. Liu et al. found an increased fatigue resistance of wrought Ti6Al4V specimens, when applying a polishing process after a shot peening procedure, although the shot peened layer will be reduced by the post-polishing process (Liu et al., 2017). In the current study, the reduction of the shot peened layer by the polishing process might have canceled out the additional fatigue advantage of the additional polishing.

4.1. Limitations

In the current study, no S-N curves were recorded, instead a Locati-test was performed, to compare the fatigue behavior of different post-treatments of LPBF manufactured specimens. This makes it difficult to compare the current results to literature. However, due to a high variety of LPBF, HIP post-processing and test parameters, comparisons of the presented own results with literature is barely possible, even with S-N curves, as the different fatigue results in literature demonstrate. As mentioned previously, cyclic tensile tests were typically used to determine the fatigue resistance. For the application of hip stems produced by AM tensile tests would not lead to purposeful results, because bending stresses are the main stresses, which typically occur in vivo. To be close to the real loading case, the four-point bending test was applied to mimic the equivalent stresses as in hip stems. Instead of a 0.1 ratio, a sinusoidal force was applied in the tensile swelling regime having a minimum of 100 N and an increasing maximum of 500 N for each load level during the Locati-test. The test conditions should again replicate the in vivo condition, where constant torque and bending stresses are acting due to muscle and ligamental forces even in a resting position. The increasing maximum forces can be associated with different activities, which lead to higher stresses at the implant. The benefit of the current study is that the LPBF processing parameters and HIP parameters remained constant and post-treatments could be directly compared using the same specimens and test conditions. Last, failure origins were analyzed for limited samples of each group. A correlation between amount or depth of compression residual stresses and the occurrence of sub-surface material failures would be valuable. However, the few analyzed samples showed, that the mechanical surface treatments inducing high residual stresses in combination with a HIP-process can lead to sub-surface failures.

4.2. Clinical relevance

The findings of this study are relevant for a wide range of applications. In the following, the clinical benefit of LPBF manufactured implants will be explained. For patients, who need a customized hip implant, the patient's bone can be reconstructed using CT data. Then, the patient-specific hip implant is designed based on 3D reconstruction of the bone and is additively manufactured (Gotze et al., 2009). Depending on the patient's age, more than 2 to 2.5 million load cycles per year act at the implant, which may lead to a fatigue failure of the implant (Kinkel et al., 2009). In addition, the hip implant must withstand high impact stresses, which occur for example during stumbling of a patient (Bergmann et al., 2004). To ensure the patient safety, post-treatments of LPBF manufactured implants would be necessary. Thereby, a previous HIP treatment needs to be applied to reduce the porosity to a minimum. Afterwards, based on the results of the current study, a shot peening process is proposed to be applied on a complex part like a (patient-specific) hip stem, to induce compressive residual stresses and to reduce the surface roughness. Next to the fatigue resistance, the hip implant needs to be osseointegrated into the surrounding bone. A high implant roughness at the stem is directly linked to a superior bone fixation (Barfeie et al., 2015). Surface roughness after shot peening in the current study was below 4 μm. The shot peened LPBF manufactured Ti6Al4V specimens in other studies ranged between 2 and 5 μm (Aguado-Montero et al., 2022; Luo et al., 2021). Subsequent to the shot peening process, a rough coating could be applied on the implants surface to improve the osseointegration. A previous study showed good adhesion of a plasma-sprayed hydroxylapatite coating on Ti6Al4V discs having a surface roughness R_a of 3.2 μm, which is similar as the roughness after shot peening in the current study (Levingstone et al., 2015). In (Yang et al., 2000), the residual stresses of plasma-sprayed hydroxylapatite coatings on Ti6Al4V specimens were analyzed and compressive residual stresses were determined. However, the effects of a

coating on the compressive residual stresses of the substrates surface, induced by the shot-peening process, needs to be evaluated. It is necessary that the compressive residual stresses on the Ti6Al4V surface are not negatively influenced by the coating process. Most hip implants have a polished shoulder and neck region, because no osseointegration is possible in this area and irritation of the surrounding soft tissue should be avoided. The current study showed that an additional polishing process after the application of a HIP process and a shot peening process is possible without any reduction in fatigue performance. In addition, the subsequent polishing process after shot peening may eliminate small crack initiation points at the highly stressed neck region of the stem.

5. Conclusion and future work

In the current study, different mechanical post-treatments of LPBF manufactured samples were tested to establish a production chain for LPBF manufactured hip stems with sufficient fatigue resistance. Thereby, the following research questions were investigated and answered.

1) Is the fatigue resistance of LPBF manufactured Ti6Al4V specimens, receiving a HIP procedure, similar to the fatigue resistance of the wrought material?
   - The herein presented results have shown, that for the chosen process parameters in combination with the cyclic four-point-bending loading, a HIP treatment without any further surface treatment is not sufficient to get a similar fatigue resistance as for specimens manufactured based on wrought Ti6Al4V material.
2) Is there a requirement to apply an additional HIP process prior to the application of mechanical surface treatments?
   - A mechanical surface treatment without a previous HIP treatment led to a lower fatigue resistance compared to specimens receiving both.
3) Which mechanical surface treatment results in a similar fatigue behavior of LPBF
   manufactured Ti6Al4V specimens as wrought material?
   - A turning, deep rolling or shot peening process led to similar fatigue results as the wrought Ti6Al4V material, when a previous HIP treatment was applied.
   - Laser shock peening or polishing led to significant lower fatigue results compared to the other mechanical surface treatments.
   - For simple geometries, a turning process or deep rolling may be appropriate, for complex shaped geometries, e.g. hip stems, shot peening represents the better choice.
4) Do near surface compressive residual stresses or a reduction of the surface roughness lead to
   a higher level of fatigue resistance?
   - A turning process, deep rolling and shot peening led to high compressive residual stresses at the specimen surface compared to laser shock peening and polishing.
   - Deep rolling had the highest depth range of the region having compressive residual stresses compared to the other surface treatments but showed the highest directional dependence.
   - In the present study laser shock peening resulted in tensile residual stresses at the very surface changing to compressive residual stresses at larger depths.
   - Polishing led to the lowest surface roughness compared to all other surface treatments.
   - From this and the fatigue results from research question 3 it can be concluded that the compressive residual stresses have a higher positive impact on the fatigue resistance than the reduction of the surface roughness.
5) Does a reduction of the surface roughness subsequent to a mechanical surface treatment further increase the fatigue resistance?
   - A combination of shot peening and polishing (regardless of the order) led to similar fatigue resistances as shot peening alone.
   - From this it can be concluded that the combination of a surface treatment leading to high compressive residual stresses and a surface treatment leading to low surface roughness does not bring any benefits nor is it harmful with regard to the fatigue behavior. But it may be beneficial for the neck region of hip implants to reduce irritation of the surrounding soft tissue and, moreover, minimize potential crack initiation points at this highly stressed hip implant region.

All these research questions are limited to the applied LPBF process, the HIP treatment and the mechanical surface treatments as well as the test conditions. Different parameters for the LPBF process, post-treatments and test conditions may lead to other results.

The study can help to develop customized hip implants, which may improve clinical outcomes without sacrificing patient safety. In a subsequent study, hip stems will be LPBF manufactured according to the established production chain selecting the optimal mechanical post-treatments. The hip implants will then be tested according to ISO 7206-4 and ISO 7206-6 to ensure patient safety for LPBF manufactured hip stems. Two more factors next to the fatigue resistance of artificial hips should be analyzed in future studies:

Firstly, the bonding strenght of the shot peened surface and a osseointegrative coating (e.g. hydroxylapatite).

Secondly, the corrosion and fretting resistance of the taper connection of the additive manufactured femoral stem.

CRediT authorship contribution statement

Stefan Schroeder: Writing – original draft, Visualization, Methodology, Investigation, Formal analysis, Data curation, Conceptualization. **Jens Gibmeier:** Writing – original draft, Visualization, Methodology, Investigation, Formal analysis, Data curation, Conceptualization. **Phuong Thao Mai:** Writing – review & editing, Visualization, Methodology, Investigation, Formal analysis, Data curation, Conceptualization. **Maximilian C.M. Fischer:** Writing – review & editing, Resources, Methodology, Investigation, Formal analysis, Data curation, Conceptualization. **Moritz M. Innmann:** Writing – review & editing, Visualization, Conceptualization. **Tobias Renkawitz:** Writing – review & editing, Visualization, Project administration, Funding acquisition, Conceptualization. **J. Philippe Kretzer:** Writing – review & editing, Visualization, Project administration, Funding acquisition, Conceptualization.

Declaration of competing interest

The authors declare the following financial interests/personal relationships which may be considered as potential competing interests:

J.P. Kretzer reports financial support was provided by German Federal Ministry of Education and Research (BMBF). J.P. Kretzer reports a relationship with DFG - German Research Foundation that includes: funding grants. J.P. Kretzer reports a relationship with German Federal Ministry of Education and Research (BMBF) that includes: funding grants. J.P. Kretzer reports a relationship with Ghent University that includes: funding grants. J.P. Kretzer reports a relationship with Stiftung Endoprothetik that includes: funding grants. J.P. Kretzer reports a relationship with German Arthrosis Aid that includes: funding grants. J. P. Kretzer reports a relationship with Endocon GmbH that includes: funding grants. J.P. Kretzer reports a relationship with Permedica S.P.A. that includes: consulting or advisory and funding grants. J.P. Kretzer reports a relationship with Implantcast GmbH that includes: funding grants. J.P. Kretzer reports a relationship with Mathys Orthopädie GmbH that includes: funding grants. J.P. Kretzer reports a relationship with AQ Solutions GmbH that includes: funding grants. J.P. Kretzer reports a relationship with CeramTec GmbH that includes: consulting or advisory and funding grants. J.P. Kretzer reports a relationship with Peter Brehm Chirurgie-Mechanik e.K. that includes: funding grants. J.P. Kretzer reports a relationship with Sintx Technologies, Inc. that

includes: funding grants. J.P. Kretzer reports a relationship with Questmed GmbH that includes: funding grants. J.P. Kretzer reports a relationship with SpineServ GmbH & Co. KG that includes: funding grants. J.P. Kretzer reports a relationship with Arbeitsgemeinschaft Endoprothetik (AE) that includes: speaking and lecture fees. J.P. Kretzer reports a relationship with Mathys Orthopaedics Ptd Ltd that includes: consulting or advisory. J.P. Kretzer reports a relationship with DePuy Synthes that includes: consulting or advisory. J.P. Kretzer reports a relationship with MedCert GmbH that includes: speaking and lecture fees. J.P. Kretzer reports a relationship with Consult Invest Beteil. GmbH that includes: consulting or advisory. T. Renkawitz reports a relationship with Arbeitsgemeinschaft Endoprothetik (AE) that includes: funding grants. T. Renkawitz reports a relationship with DGOU that includes: funding grants. T. Renkawitz reports a relationship with German Society for Orthopaedics and Orthopaedic Surgery that includes: board membership and funding grants. T. Renkawitz reports a relationship with BVOU that includes: funding grants. T. Renkawitz reports a relationship with DePuy International Ltd that includes: funding grants. T. Renkawitz reports a relationship with Otto Bock Foundation that includes: funding grants. T. Renkawitz reports a relationship with German Arthrosis Aid that includes: funding grants. T. Renkawitz reports a relationship with Aesculap AG that includes: funding grants. T. Renkawitz reports a relationship with Zimmer Biomet that includes: funding grants. T. Renkawitz reports a relationship with Oskar Helene Home Foundation that includes: funding grants. T. Renkawitz reports a relationship with Vielberth Foundation that includes: funding grants. T. Renkawitz reports a relationship with German Ministry of Education and Research that includes: funding grants. T. Renkawitz reports a relationship with German Federal Ministry of Economic Cooperation and Development that includes: funding grants. T. Renkawitz reports a relationship with Die Orthopädie that includes: board membership. T. Renkawitz reports a relationship with Die Unfallchirurgie that includes: board membership. T. Renkawitz reports a relationship with OUMN that includes: board membership. T. Renkawitz reports a relationship with AAOS that includes: board membership. M.C.M. Fischer reports a relationship with AQ Solutions GmbH that includes: employment. S. Schroeder reports a relationship with German Arthrosis Aid that includes: funding grants. If there are other authors, they declare that they have no known competing financial interests or personal relationships that could have appeared to influence the work reported in this paper.

Acknowledgments

This research and development project was funded by the German Federal Ministry of Education and Research (BMBF) within the “The Future of Value Creation – Research on Production, Services and Work” program (funding number 02P18C002) and managed by the Project Management Agency Karlsruhe (PTKA). The authors are responsible for the content of this publication. The authors would like to thank the EOS GmbH (Krailingen, Germany) for guidance regarding the printing process and the HIP treatment and finding the optimum AM process parameters that could have appeared to influence the work reported in this paper. We would also like to thank Mr. Stephan Kuhlmann of Curtiss-Wright, Metal Improvement Company, Surface Technologies in Unna, Germany, for performing the shot peening treatment.

Data availability

Data will be made available on request.

References

Aguado-Montero, S., Navarro, C., Vázquez, J., Lasagni, F., Slawik, S., Domínguez, J., 2022. Fatigue behaviour of PBF additive manufactured TI6AL4V alloy after shot and laser peening. Int. J. Fatig. 154.

Alegre, J.M., Díaz, A., García, R., Peral, L.B., Cuesta, I.I., 2022. Effect of HIP post-processing at 850 °C/200 MPa in the fatigue behavior of Ti-6Al-4V alloy fabricated by Selective Laser Melting. Int. J. Fatig. 163.

Altenberger, I., Nalla, R.K., Sano, Y., Wagner, L., Ritchie, R.O., 2012. On the effect of deep-rolling and laser-peening on the stress-controlled low- and high-cycle fatigue behavior of Ti–6Al–4V at elevated temperatures up to 550°C. Int. J. Fatig. 44, 292–302.

Australian Orthopaedic Association, 2022. Annual report. https://aoanjrr.sahmri.com/de/annual-reports-2022. December, 2022.

Barfeie, A., Wilson, J., Rees, J., 2015. Implant surface characteristics and their effect on osseointegration. Br. Dent. J. 218, E9.

Benedetti, M., Torresani, E., Leoni, M., Fontanari, V., Bandini, M., Pederzolli, C., Potrich, C., 2017. The effect of post-sintering treatments on the fatigue and biological behavior of Ti-6Al-4V ELI parts made by selective laser melting. J. Mech. Behav. Biomed. Mater. 71, 295–306.

Benzing, J., Hrabe, N., Quinn, T., White, R., Rentz, R., Ahlfors, M., 2019. Hot isostatic pressing (HIP) to achieve isotropic microstructure and retain as-built strength in an additive manufacturing titanium alloy (Ti-6Al-4V). Mater. Lett. 257.

Bergmann, G., Graichen, F., Rohlmann, A., 2004. Hip joint contact forces during stumbling. Langenbecks Arch. Surg. 389, 53–59.

Chen, Q., Thouas, G.A., 2015. Metallic implant biomaterials. Mater. Sci. Eng. R Rep. 87, 1–57.

Chen, S.Y., Huang, J.C., Pan, C.T., Lin, C.H., Yang, T.L., Huang, Y.S., Ou, C.H., Chen, L.Y., Lin, D.Y., Lin, H.K., Li, T.H., Jang, J.S.C., Yang, C.C., 2017. Microstructure and mechanical properties of open-cell porous Ti-6Al-4V fabricated by selective laser melting. J. Alloys Compd. 713, 248–254.

Chen, G., Muheremu, A., Yang, L., Wu, X., He, P., Fan, H., Liu, J., Chen, C., Li, Z., Wang, F., 2020. Three-dimensional printed implant for reconstruction of pelvic bone after removal of giant chondrosarcoma: a case report. J. Int. Med. Res. 48, 300060520917275.

Dall’Ava, L., Hothi, H., Henckel, J., Di Laura, A., Tirabosco, R., Eskelinen, A., Skinner, J., Hart, A., 2021. Osseointegration of retrieved 3D-printed, off-the-shelf acetabular implants. Bone & joint research 10, 388–400.

Dall’Ava, Hothi, Di, L., Henckel, Hart, 2019. 3D Printed Acetabular Cups for Total Hip Arthroplasty: a Review Article. Metals 9.

Edwards, P., Ramulu, M., 2014. Fatigue performance evaluation of selective laser melted Ti–6Al–4V. Mater. Sci. Eng., A 598, 327–337.

Gotze, C., Rosenbaum, D., Hoedemaker, J., Bottner, F., Steens, W., 2009. Is there a need of custom-made prostheses for total hip arthroplasty? Gait analysis, clinical and radiographic analysis of customized femoral components. Arch. Orthop. Trauma Surg. 129, 267–274.

Hertz, H., 1882. Ueber die Berührung fester elastischer Körper. J. für die Reine Angewandte Math. (Crelle’s J.) 156–171.

von Hertzberg-Boelch, S.P., Wagenbrenner, M., Arnholdt, J., Frenzel, S., Holzapfel, B.M., Rudert, M., 2021. Custom made monoflange acetabular components for the treatment of paprosky type III defects. J Pers Med 11.

Jiang, Q., Li, S., Zhou, C., Zhang, B., Zhang, Y., 2021. Effects of laser shock peening on the ultra-high cycle fatigue performance of additively manufactured Ti6Al4V alloy. Opt Laser. Technol. 144.

Jin, Y.Z., Zhao, B., Lu, X.D., Zhao, Y.B., Zhao, X.F., Wang, X.N., Zhou, R.T., Qi, D.T., Wang, W.X., 2021. Mid- and long-term Follow-Up efficacy analysis of 3D-Printed interbody fusion cages for anterior cervical discectomy and fusion. Orthop. Surg. 13, 1969–1978.

Jurg, M., Medvedev, A.E., Yan, W., Molotnikov, A., 2022. Surface improvement of laser powder bed fusion processed Ti6Al4V for fatigue applications. Additive Manufacturing Letters 3.

Kahlin, M., Ansell, H., Basu, D., Kerwin, A., Newton, L., Smith, B., Moverare, J.J., 2020. Improved fatigue strength of additively manufactured Ti6Al4V by surface post processing. Int. J. Fatig. 134.

Kasperovich, G., Hausmann, J., 2015. Improvement of fatigue resistance and ductility of TiAl6V4 processed by selective laser melting. J. Mater. Process. Technol. 220, 202–214.

Kinkel, S., Wollmerstedt, N., Kleinhans, J.A., Hendrich, C., Heisel, C., 2009. Patient activity after total hip arthroplasty declines with advancing age. Clin. Orthop. Relat. Res. 467, 2053–2058.

Kumar, P., Ramamurty, U., 2020. High cycle fatigue in selective laser melted Ti-6Al-4V. Acta Mater. 194, 305–320.

Lal, H., Patralekh, M.K., 2018. 3D printing and its applications in orthopaedic trauma: a technological marvel. Journal of clinical orthopaedics and trauma 9, 260–268.

Leuders, S., Thöne, M., Riemer, A., Niendorf, T., Tröster, T., Richard, H.A., Maier, H.J., 2013. On the mechanical behaviour of titanium alloy TiAl6V4 manufactured by selective laser melting: fatigue resistance and crack growth performance. Int. J. Fatig. 48, 300–307.

Levingstone, T.J., Ardhaoui, M., Benyounis, K., Looney, L., Stokes, J.T., 2015. Plasma sprayed hydroxyapatite coatings: understanding process relationships using design of experiment analysis. Surf. Coating. Technol. 283, 29–36.

Lin, Y.-C., Zhu, J.-S., Chen, J.-Y., Wang, J.-Q., 2021. Residual-stress relaxation mechanism and model description of 5052H32 Al alloy spun ellipsoidal heads during annealing treatment. Advances in Manufacturing 10, 87–100.

Liu, Y., Yang, Y., Wang, D., 2016. A study on the residual stress during selective laser melting (SLM) of metallic powder. Int. J. Adv. Des. Manuf. Technol. 87, 647–656.

Liu, Z.G., Wong, T.I., Huang, W., Sridhar, N., Wang, S.J., 2017. Effect of surface polishing treatment on the fatigue performance of shot-peened Ti–6Al–4V alloy. Acta Metall. Sin. 30, 630–640.

Liu, F., Xie, H., He, W., 2023. Multi-field coupling fatigue behavior of laser additively manufactured metallic materials: a review. J. Mater. Res. Technol. 22, 2819–2843.

Luo, X., Dang, N., Wang, X., 2021. The effect of laser shock peening, shot peening and their combination on the microstructure and fatigue properties of Ti-6Al-4V titanium alloy. Int. J. Fatig. 153.
Masuo, H., Tanaka, Y., Morokoshi, S., Yagura, H., Uchida, T., Yamamoto, Y., Murakami, Y., 2018. Influence of defects, surface roughness and HIP on the fatigue strength of Ti-6Al-4V manufactured by additive manufacturing. Int. J. Fatig. 117, 163–179.
Mertova, K., Džugan, J., Roudnicka, M., 2018. Fatigue properties of SLM-produced Ti6Al4V with various post-processing processes. IOP Conf. Ser. Mater. Sci. Eng. 461, 012052.
Nguyen, D.S., Park, H.S., Lee, C.M., 2020. Optimization of selective laser melting process parameters for Ti-6Al-4V alloy manufacturing using deep learning. J. Manuf. Process. 55, 230–235.
Parry, L., Ashcroft, I.A., Wildman, R.D., 2016. Understanding the effect of laser scan strategy on residual stress in selective laser melting through thermo-mechanical simulation. Addit. Manuf. 12, 1–15.
Parry, L.A., Ashcroft, I.A., Wildman, R.D., 2019. Geometrical effects on residual stress in selective laser melting. Addit. Manuf. 25, 166–175.
Pegues, J., Roach, M., Scott Williamson, R., Shamsaei, N., 2018. Surface roughness effects on the fatigue strength of additively manufactured Ti-6Al-4V. Int. J. Fatig. 116, 543–552.
du Plessis, A., 2019. Effects of Process Parameters on Porosity in Laser Powder Bed Fusion Revealed by X-ray Tomography. Additive Manufacturing 30.
du Plessis, A., Macdonald, E, 2020. Hot isostatic pressing in metal additive manufacturing: X-ray tomography reveals details of pore closure. Addit. Manuf. 34.
Qiu, C., Adkins, N.J.E., Attallah, M.M., 2013. Microstructure and tensile properties of selectively laser-melted and of HIPed laser-melted Ti–6Al–4V. Mater. Sci. Eng., A 578, 230–239.
Ren, B., Wan, Y., Liu, C., Wang, H., Yu, M., Zhang, X., Huang, Y., 2021. Improved osseointegration of 3D printed Ti-6Al-4V implant with a hierarchical micro/nano surface topography: an in vitro and in vivo study. Materials science & engineering. C, Materials for biological applications 118, 111505.
Sadoghi, P., Pawelka, W., Liebensteiner, M.C., Williams, A., Leithner, A., Labek, G., 2014. The incidence of implant fractures after total hip arthroplasty. Int. Orthop. 38, 39–46.
Shui, X., Yamanaka, K., Mori, M., Nagata, Y., Kurita, K., Chiba, A., 2017. Effects of post-processing on cyclic fatigue response of a titanium alloy additively manufactured by electron beam melting. Mater. Sci. Eng., A 680, 239–248.
Snow, Z., Cummings, C., Reutzel, E.W., Nassar, A., Abbot, K., Guerrier, P., Kelly, S., McKown, S., Blecher, J., Overdorff, R., 2023. Analysis of factors affecting fatigue performance of HIP'd laser-based powder bed fusion Ti–6Al–4V coupons. Mater. Sci. Eng., A 864.
Sonntag, R., Reinders, J., Gibmeier, J., Kretzer, J.P., 2015. Fatigue performance of medical Ti6Al4V alloy after mechanical surface treatments. PLoS One 10, e0121963.
Sonntag, R., Gibmeier, J., Pulvermacher, S., Mueller, U., Eckert, J., Braun, S., Reichkendler, M., Kretzer, J.P., 2019. Electrocautery damage can reduce implant fatigue strength: cases and in vitro investigation. The Journal of bone and joint surgery. American 101, 868–878.
Strantza, M., Vafadari, R., de Baere, D., Vrancken, B., van Paepegem, W., Vandendael, I., Terryn, H., Guillaume, P., van Hemelrijck, D., 2016. Fatigue of Ti6Al4V structural health monitoring systems produced by selective laser melting. Materials 9.
Strantza, M., Ganeriwala, R.K., Clausen, B., Phan, T.Q., Levine, L.E., Pagan, D., King, W. E., Hodge, N.E., Brown, D.W., 2018. Coupled experimental and computational study of residual stresses in additively manufactured Ti-6Al-4V components. Mater. Lett. 231, 221–224.
Wang, H., Zhao, B., Liu, C., Wang, C., Tan, X., Hu, M., 2016. A comparison of biocompatibility of a titanium alloy fabricated by Electron beam melting and selective laser melting. PLoS One 11, e0158513.
Wixted, C.M., Peterson, J.R., Kadakia, R.J., Adams, S.B., 2021. Three-dimensional printing in orthopaedic surgery: current applications and future developments. J Am Acad Orthop Surg Glob Res Rev 5, e20 00230–211.
Wolfstieg, U., 1976. Die Symmetrisierung unsymmetrischer Interferenzlinien mit Hilfe von Spezialblenden. Härt.-Tech. Mittl. 31, 23–27.
Wycisk, E., Emmelmann, C., Siddique, S., Walther, F., 2013. High Cycle Fatigue (HCF) performance of Ti-6Al-4V alloy processed by selective laser melting. Adv. Mater. Res. 134–139, 816-817.
Xu, Z., Liu, A., Wang, X., 2022. Fatigue performance differences between rolled and selective laser melted Ti6Al4V alloys. Mater. Char. 189.
Yang, Y.C., Chang, E., Hwang, B.H., Lee, S.Y., 2000. Biaxial residual stress states of plasma-sprayed hydroxyapatite coatings on titanium alloy substrate. Biomaterials 21, 1327–1337.
Zhao, X., Li, S., Zhang, M., Liu, Y., Sercombe, T.B., Wang, S., Hao, Y., Yang, R., Murr, L. E., 2016. Comparison of the microstructures and mechanical properties of Ti–6Al–4V fabricated by selective laser melting and electron beam melting. Mater. Des. 95, 21–31.